

Characteristics Exploration of NiCuZn Nano-Composite coated Permanent Magnets

T. Narasimhulu, Mallikarjuna Rao Pasumarthi

Department of Electrical Engineering, Andhra University College of Engineering (A), Andhra University, Visakhapatnam, India

Abstract—This paper presents the synthesis of $Ni_{0.5}Cu_{0.2}Zn_{0.3}Fe_2O_4$ compound using Citrate Precursor Sol- Gel Method and Ball milling for grinding the compound. X-ray diffraction measurements (XRD) confirmed the formation of single-phase cubic spinel structure. The average crystallite size was calculated using XRD pattern and confirmed by Scanning Electron Microscope (SEM). The electromagnetic properties were investigated using Vector Network Analyzer (VNA) and molar magnetic susceptibility measurements. The magnetic measurements have proved that the entire preparation method has considerable effect in enhancing the magnetic properties of the system. And an application of PMLDC machine design with ferrite coated permanent magnets having competitive power density and efficiency. The influence of temperature variation on the magnets on the electric machine performance is also observed.

Keywords— ferrite coat; magnetic susceptibility; Citrate Precursor Sol- Gel Method; Ball Milling.

I. INTRODUCTION

At present surface-mounting devices have been developed for electronic applications, which are produced by coating ferrite and Ag electrode layers alternately and co-firing them. Low temperature sintered NiCuZn ferrites are the most universal ferrite materials to produce MLCIs because of their relatively low sintering temperature and high resistivity with good performances in the high frequency range [1–3]. Typical NiCuZn ferrites with a regular particle size have sintering temperatures above 1000°C. The usage of fine powder decreases the sintering temperature of ferrites. Fine powders can be prepared through various wet-chemical methods like co-precipitation [4], hydrothermal synthesis [5] and sol-gel processes [6]. Although the co-precipitation and sol-gel methods are the most popular, they have some disadvantages as most of them are highly pH sensitive and require special attention for complex systems whereas the sol-gel technique requires expensive alkoxide precursor material and stringent process of gel product [7]. Among the established synthetic methods, it is still

critical to find simple and cost-effective routes to synthesize nano-crystalline NiCuZn ferrites by using cheap, nontoxic and environmentally benign precursors. In addition to their high nutrition quality egg-white proteins are well known for their gelling, foaming and emulsifying characteristics [8-9]. NiCuZn ferrites of composition $Ni_{0.7-x}Cu_xZn_{0.3}Fe_2O_4$ ($x = 0, 0.2, 0.4, 0.6$) prepared by citrate precursor method, characteristics are investigated and reported [10]. X-ray diffraction (XRD) confirmed the formation of single-phase cubic spinel structure. The grain size, estimated by SEM micrograph, was found to increase with Cu content. The hysteresis data indicated that the maximum saturation magnetization was obtained for the composition with $x = 0.2$. Lima [11] synthesized $Ni_xCu_{0.5-x}Zn_{0.5}Fe_2O_4$ ferrite ($0.2 \leq x \leq 0.4$) nano-particles using the citrate precursor method. Vibrating sample magnetometer (VSM) showed that adding copper to NiZn ferrite decreases magnetization saturation and the calcining temperature. Ferrites with compositions of $Ni_{0.27}Zn_{0.64}Cu_xFe_{1.98}O_4$ ($x = 0.1, 0.2$) were prepared by conventional ceramic methods [12]. The intergranular pores in the prepared ferrites were found to generate large demagnetizing fields, reduce the temperature dependence of the effective anisotropy field and thus decrease the temperature dependence of the relative initial permeability. Fine powders of $Ni_{0.6-x}Cu_xZn_{0.4}Fe_2O_4$, where $0 \leq x \leq 0.4$ were prepared by the citrate precursor method [13]. XRD confirmed the formation of single-phase cubic spinel structure. The addition of copper was found to promote the grain growth, resulting in an increase in the grain size. Curie temperature, however, was understandably lowered with the increase in Cu content. Ferrite with Cu concentration of $x = 0.4$, showed the highest value of initial permeability.

In the present paper, synthesis of NiCuZn ferrites by a simple method uses Citrate Precursor Sol- Gel Method and Ball milling for grinding the compound. The synthesized nanocrystals have been characterized using thermal analysis techniques. Calcined nano-ferrite samples are characterized by X-ray diffraction (XRD) and Scanning Electron Microscopy (SEM). The magnetic properties of the ferrites

were investigated using a Vector Network Analyzer (VNA) at room temperature and magnetic susceptibility measured at different magnetic fields and temperatures.

Permanent magnet technology is constantly developing. At present NdFeB magnets are being used in electrical machines. Due to their cost and low availability alternatives are being explored. An additional boost of the progress of permanent magnet synchronous machines (PMSMs) was got after establishing of the interior magnet rotor structure [14], [15] and with the development of tooth-coil winding approaches [16], [17]. [18] presents, At this power and speed areas conventional asynchronous machines should have similar performance characteristics as PMSMs with slightly smaller peak efficiency in the static efficiency map, less torque density and lower power factor [19]. After the rapid increase of the neodymium magnets' price in 2010, there appeared many companies and organizations searching for appropriate designs for so called "rare earth free" electric machines. The main purpose of the rare earth free electric machines is to reach almost the same torque density as in commercially available neodymium PMSMs, without efficiency deterioration. Major part of these attempts is done for hybrid electric vehicle applications [20-27]. Common measures in order to increase the power density of PMSMs are high angular speeds [28], increase the number of pole pairs and increasing the tangential stress [29].

This paper narrates the possibilities for improving the torque density with the use of ferrite coat on magnetic surface of PMBLDC machine. Permanent-magnet (PM) BLDC motor with rare-earth PMs is most popular, but rare-earth PMs have problems with high power low voltage applications, high cost and limited supply. Therefore, the electric motors with less or no rare-earth permanent magnets are available for numerous application.

II. SYNTHESIS OF NANO-COMPOUND

This section gives the details of synthesis of the nano compound $Ni_{0.5}Cu_{0.2}Zn_{0.3}Fe_2O_4$:

- A magnetic spinel nano NiCuZn ferrite catalyst with composition $Ni_{0.5}Cu_{0.2}Zn_{0.3}Fe_2O_4$ was chosen for this study.
- For the preparation of catalyst, aqueous solutions of stoichiometric amounts of Nickel nitrate, Copper nitrate and Zinc nitrate along with ferric citrate were reacted with citric acid in 1:1 molar ratio.
- pH of the solution was increased by the addition of ammonia to complete the reaction and ethane diol was added.

- The solution was evaporated very slowly over a period of 24 hours to dryness. Viscosity and color were changed as the solution turned into puffy, porous dry gel. As soon as the solvent removal is completed, dried precursor goes under a self-ignition reaction to form a very fine powder known as synthesized powder.
- The synthesized powder thus obtained was calcined in a muffle furnace at 600c for 2 hours to remove the residual carbon and furnace cooled. Then matter is subjected to Ball milling for 2 hours at speed of 450 rpm.

III. CHARACTERIZATION OF NANO COPPER FERRITE

a. X- RAY DIFFRACTION (XRD) ANALYSIS:

Fig1. shows typical XRD pattern for nano copper ferrite sample which was sintered at 600 degree celsius. The pattern shows all the characteristics peaks of a spinel structure and confirms the phase formation indicating the absence of other impurity phases. The XRD parameters of various peaks were compared with the standard data of the cubic copper ferrites and found to be in cubic phase. The particle size and other characteristics of the copper nano particles obtained from the XRD pattern using Scherrer's formula was found to be 39nm and reported in table1. The peaks can be indexed to (220),(311),(400),(422),(511) and (440) phases of a cubic unit cell are shown in fig 2. The X-ray diffraction pattern was studied in detail for the determination of crystallite size by using the classical Scherrer equation [15]:

$$D = \frac{k\lambda}{\beta \cos\theta} \quad (1)$$

Where, D is the average crystallite size, k is a constant equal to 0.89, λ is the X-ray wave length (0.1542 nm), θ is the angle of diffraction and β is the full width at half maximum (FWHM) of the peak.

The average crystallite sizes of the powders were in the range 39 nm which indicates that the Cu substitution for Ni has no effect on the crystal size.

The lattice parameter (a) has been calculated from X-ray data using the formula:

$$\frac{1}{d^2} = \frac{h^2 + k^2 + l^2}{a^2} \quad (2)$$

Where, d is the lattice spacing and h, k and l are the miller indices of the plane.

The theoretical density or the X-ray density (D_x) was calculated according to relation:

$$D_x = \frac{ZM}{Na^3} \quad (3)$$

The variation of the average crystallite size, lattice parameter and X-ray density, with copper content, are shown in Table 1.

Where, Z is the number of molecules per unit cell (Z = 8), M is the molecular weight, N is Avogadro's number and a^3 is the volume of unit cell.

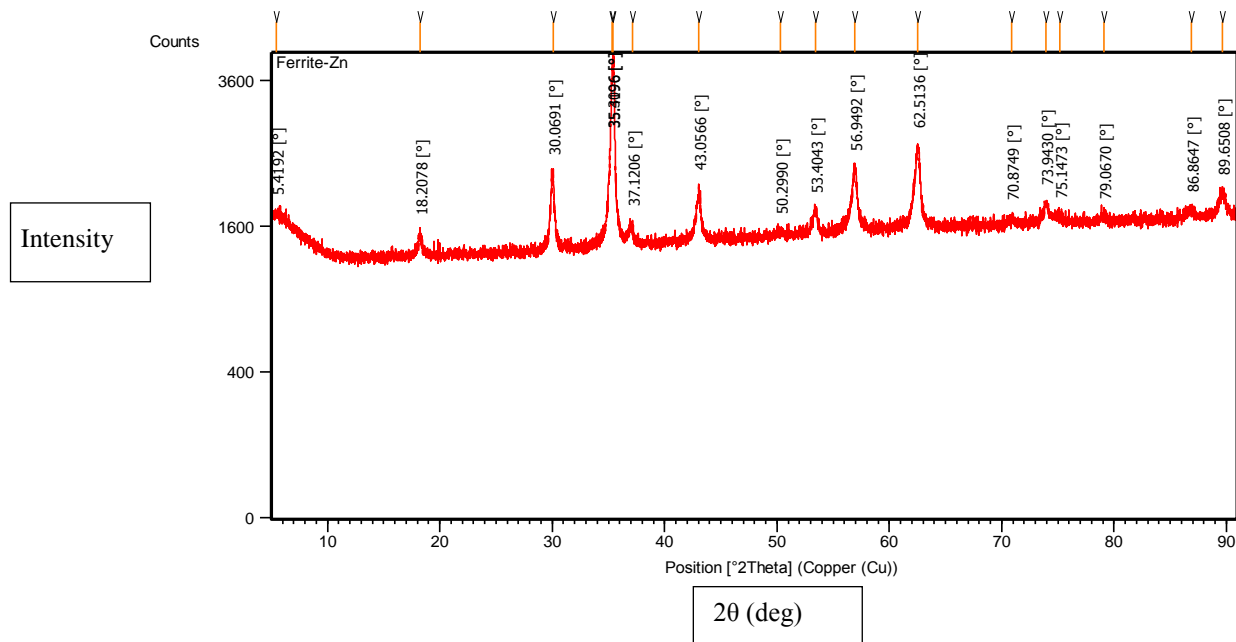


Fig.1: XRD Pattern of Nano-Composite $Ni_{0.5}Cu_{0.2}Zn_{0.3}Fe_2O_4$

b. Morphological and elemental analysis (SEM&EDS):

Fig3 shows the typical SEM image of the nano NiCuZn ferrite sintered at 600 degree Celsius. The crystallite size calculated from XRD is in the range of below 30 nm which is in agreement with the SEM image. The structural composition and crystallinity of the NiCuZn ferrite nano particles was further examined by using SEM and TEM. The iron and copper ratio in the nano crystals as determined by EDX analysis was very much close to the atomic ratio in the formula NiCuZn ferrite.

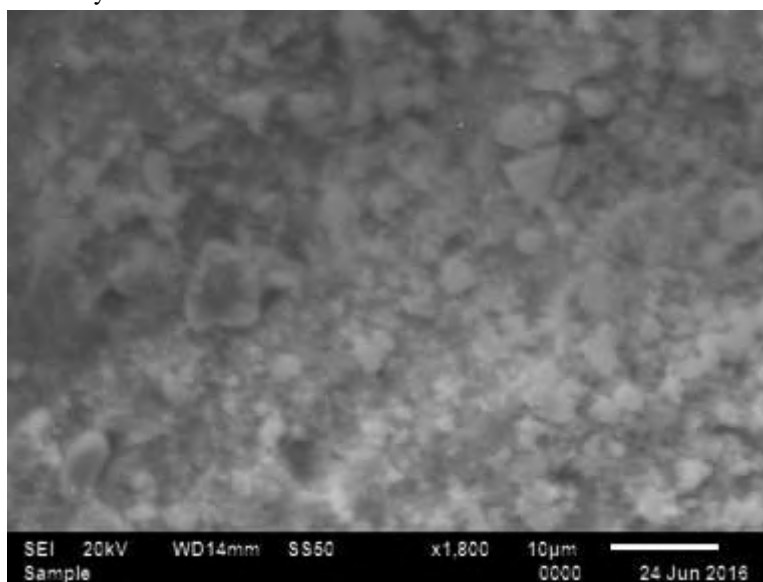


Fig.3: Obtained SEM image of NiCuZn ferrite

Table.1: particle size and other characteristics of the nano $Ni_{0.5}Cu_{0.2}Zn_{0.3}Fe_2O_4$ ferrite obtained from the XRD analysis.

S. NO	Parameters	Values
1	Lattice parameter (a)	8.379 Å
2	Density (%)	94.2
3	X-ray density (D_x)	5.35g/m
4	FWHM	0.284
5	Grain size	1.42
6	Average crystallite size (D)	39 nm
7	Saturation magnetization (M_s)	47.4 emu/g
8	Magnetic moment (η_B)	2.03 μ_B
9	Remnant magnetization, M_r	7.15 emu/g
10	Corecivity, H_c	67.8 Oe
11	Curie Temperature, T_c	690 °C
12	Effective magnetic moment (μ_{eff})	4.65 μ_B

IV. RESULTS AND DISCUSSION

Electromagnetic properties measurement of $Ni_{0.5}Cu_{0.2}Zn_{0.3}Fe_2O_4$ system is using a Vector Network Analyzer(VNA). Fig. 3 SEM image of the sample with a field scan up to ± 5.0 kOe at room temperature. The hysteresis loop of $Ni_{0.5}Cu_{0.2}Zn_{0.3}Fe_2O_4$ is shown in fig.4. The sample shows a ferromagnetic nature with curves typical for soft-magnetic materials. The values of saturation magnetization (M_s), remnant magnetization (M_r) and coercivity (H_c) are shown in Table 1. In ferrites, the magnetic moment arises mainly from the parallel uncompensated electron spin of individual ion. The intensity of magnetization can thus be explained by considering the metal ion distribution and antiparallel spin alignment of the two sub lattice sites as given by Neel's Model [19]. According to Neel's model, three types of interactions AA, AB and BB are present with the intersub-lattice AB superexchange interaction is the strongest one of them. Since Zn^{2+} ions are non-magnetic, the contribution to the magnetization is mostly due to Ni^{2+} , Cu^{2+} and Fe^{3+} ions having magnetic moments of 2.3, 1.3 and 5 μ_B respectively. The experimental magnetic moment (η_B) is determined from the saturation magnetization data using the following formula [14]:

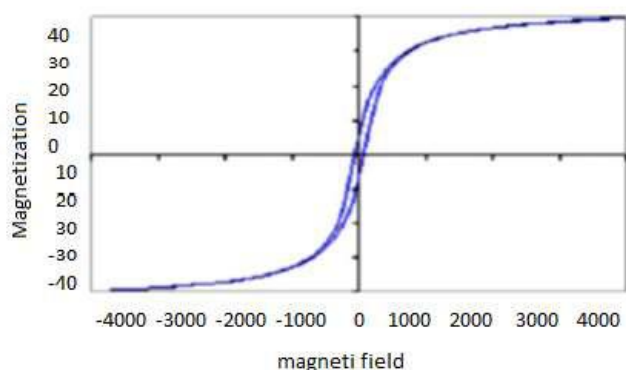
$$\eta_B = \frac{MW_x M_s}{5585} \quad (4)$$

Where MW is the molecular weight of the sample M_s is the saturation magnetization in emu/g The calculated values of the experimental magnetic moment (η_B) is presented in Table 1. The gradual decrease in the values of saturation magnetization and experimental magnetic moments with increasing copper content is accounted for the weakening of the AB interaction, which holds well with the decrease in theoretical values of magnetic moment. The decrease in coercivity (H_c) with increasing copper concentration may be attributed to lower magneto-crystalline anisotropy of Cu^{2+} ions as compared to Ni^{2+} that leads to lower coercivity according to the Stoner-Wolfforth model for coercivity of nano-particles [21].

Saturation magnetization value is obtained at room temperature is tabulated in Table 1 are relatively high especially at higher concentrations of copper content as compared with the results of Jadhav et al. [10]. On the other hand, the obtained coercivities show lower values as compared with the same results. This suggests that, the present method of synthesis used is Citrate Precursor Sol-Gel Method and Ball milling for grinding the compound, has an impact on improving the magnetic properties of the system. The temperature dependence of the molar magnetic susceptibility (χ), as a function of the magnetic field intensity is investigated for sample. The Curie temperatures and the effective magnetic moments are reported in Table 1.

Table.2: Comparison of Permanent Magnet Materials:

Material	Remanence B _r (T)	Coercivity H _c (kA/m)	Curie temperature (°C)	Comparisons
$Ni_{0.5}Cu_{0.2}Zn_{0.3}Fe_2O_4$	0.5...1.35	33.1...76.8	550...850	+ low Cost material +High magnetic properties +linear +Availability
SmCo	0.9...1.1	700...2400	500...850	+ High magnetic properties + linear + very High Cost
NdFeB	1.0...1.4	900...3200	310	+ High magnetic properties + linear -High temperature Coefficients -prone to corrosion

Fig.4: Magnetic hysteresis loops for $Ni_{0.5}Cu_{0.2}Zn_{0.3}Fe_2O_4$

For all the samples, the absence of any thermal stability of η_M with increasing temperature indicates that the thermal energy is quite sufficient to disturb the ordered spins even at lower temperatures. The measured Curie temperature decreases with increasing Cu content (Table 1). This observed variation can be explained in terms of the magnetic super exchange interaction which has a direct relation with Curie temperature [13,22]. Further, the strength of A-B interaction, which is the interaction existing between the antiparallel uncompensated electron spin of A and B sublattices is the most dominant [23]. This interaction is observed to decrease with Cu substitution as indicated by the magnetization measurements thus accounting for the fall in Curie temperature.

V. CONCLUSION

Nano-crystalline $Ni_{0.5}Cu_{0.2}Zn_{0.3}Fe_2O_4$ was successfully synthesized and prepared using Citrate Precursor Sol-Gel Method and Ball milling for grinding the compound. The obtained powders were characterized using TG, XRD, FT-IR and TEM techniques. The results indicate that, single

phase cubic ferrites were obtained after calcining the precursors at 600°C for 2 hours. On investigation of characteristics and properties it is observed that, instead of the copper substitution has weak effect on the structural properties of the system, but it greatly affects the magnetic properties. PMBLDC machine with ferrite coated magnets is simulated and its performances have been evaluated.

REFERENCES

- [1]. H. Su, H. Zhang, X. Tang, B. Liu, Z. Zhong, J. Alloys Compd. 475 (2009) 683.
- [2]. M.L.S. Teo, L.B. Kong, Z.W. Li, G.Q. Lin, Y.B. Gan, J. Alloys Compd. 459 (2008) 567.
- [3]. L.B. Kong, M.L.S. Teo, Z.W. Li, G.Q. Lin, Y.B. Gan, J. Alloys Compd. 459 (2008) 576.
- [4]. J. Kim, C. Ham, Mater. Res. Bull. 44 (2009) 633.
- [5]. K. Sadhana, K. Praveena, S. Bharadwaj, S.R. Murthy, J. Alloys Compd. 472 (2009) 484.
- [6]. M.R. Barati, J. Magn. Mater. 233 (2001) 224.
- [7]. P.K. Roy, J. Bera, J. Mater. Process. Technol. 197 (2008) 279.
- [8]. Y. Mine, Trends Food Sci. Technol. 6 (1995) 225.
- [9]. S. Maensiri, C. Masingboon, B. Boonchom, S. Seraphin, Scripta Mater. 56 (2007) 797.
- [10]. P.A. Jadhav, R.S. Devan, Y.D. Kolekar, B.K. Chougule, J. Phys. Chem. Sol. 70 (2009) 396.
- [11]. U. Lima, M. Nasara, R. Nasara, M. Rezende, J. Araujo, J. Oliveira, Mater. Sci. Eng. B 151 (2009) 238.
- [12]. J. Hu, M. Yan, W. Luo, J. Wu, Physica B 400 (2007) 119.
- [13]. M. Dimri, A. Verma, S. Kashyap, D. Dube, O. Thakur, C. Prakash, Mater. Sci. Eng. B 133 (2006) 42.

- [14]. N. Bianchi and S. Bolognani, "Influence of rotor geometry of an ipmmotor on sensorless control feasibility," *Industry Applications, IEEE Transactions on*, vol. 43, no. 1, pp. 87–96, 2007.
- [15]. R. Dutta, L. Chong, and M. Rahman, "Design and experimental verification of an 18-slot/14-pole fractional-slot concentrated winding interior permanent magnet machine," *Energy Conversion, IEEE Transactions on*, vol. 28, no. 1, pp. 181–190, 2013.
- [16]. A. EL-Refaie, "Fractional-slot concentrated-windings synchronous permanent magnet machines: Opportunities and challenges," *Industrial Electronics, IEEE Transactions on*, vol. 57, no. 1, pp. 107–121, 2010.
- [17]. P. Ponomarev, P. Lindh, and J. Pyrhonen, "Effect of slot and pole combination on the leakage inductance and the performance of tooth-coil permanent-magnet synchronous machines," pp. 1–1, 2012.
- [18]. A. Bazzi and P. Krein, "Comparative evaluation of machines for electric and hybrid vehicles based on dynamic operation and loss minimization," in *Energy Conversion Congress and Exposition (ECCE), 2010 IEEE, 2010*, pp. 3345–3351.
- [19]. R. Lateb, N. Takorabet, F. Meibody-Tabar, A. Mirzaian, J. Enon, and A. Sarribouette, "Performances comparison of induction motors and surface mounted pm motor for pod marine propulsion," in *Industry Applications Conference, 2005. Fourtieth IAS Annual Meeting. Conference Record of the 2005*, vol. 2, 2005, pp. 1342–1349 Vol. 2.
- [20]. M. Obata, S. Morimoto, M. Sanada, and Y. Inoue, "Characteristic of pmasynrm with ferrite magnets for ev/hev applications," in *Electrical Machines and Systems (ICEMS), 2012 15th International Conference on*, Oct., pp. 1–6.
- [21]. K. Chiba, S. Chino, M. Takemoto, and S. Ogasawara, "Fundamental analysis for a ferrite permanent magnet axial gap motor with coreless rotor structure," in *Electrical Machines and Systems (ICEMS), 2012 15th International Conference on*, Oct., pp. 1–6.
- [22] D. Dorrell, M.-F. Hsieh, and A. Knight, "Alternative rotor designs for high performance brushless permanent magnet machines for hybridelectric vehicles," *Magnetics, IEEE Transactions on*, vol. 48, no. 2, pp.835–838, Feb. 2012.
- [22]. S. Chino, S. Ogasawara, T. Miura, A. Chiba, M. Takemoto, and N. Hoshi, "Fundamental characteristics of a ferrite permanent magnet axial gap motor with segmented rotor structure for the hybrid electricvehicle," in *Energy Conversion Congress and Exposition (ECCE), 2011 IEEE, Sept.*, pp. 2805–2811.
- [23]. M. Paradkar and J. Boecker, "Design of a high performance ferritemagnet-assisted synchronous reluctance motor for an electric vehicle," in *IECON 2012 - 38th Annual Conference on IEEE Industrial Electronics Society*, Oct., pp. 4099–4103.
- [24]. Y.-H. Jeong, K. Kim, Y.-J. Kim, B.-S. Park, and S.-Y. Jung, "Design characteristics of pma-synrm and performance comparison with ipmsmbased on numerical analysis," in *Electrical Machines (ICEM), 2012 XXth International Conference on*, Sept., pp. 164–170.
- [25]. P. Sekerak, V. Hrabovcova, J. Pyrhonen, S. Kalamen, P. Rafajdus, and M. Onufer, "Comparison of synchronous motors with different permanent magnet and winding types," *Magnetics, IEEE Transactions on*, vol. 49, no. 3, pp. 1256–1263, March 2013.
- [26]. I. Petrov and J. Pyrhonen, "Performance of low-cost permanent magnet material in pm synchronous machines," *Industrial Electronics, IEEE Transactions on*, vol. 60, no. 6, pp. 2131–2138, June 2013.
- [27]. D. Gerada, A. Mebarki, and C. Gerada, "Optimal design of a high speed concentrated wound pmsm," in *Electrical Machines and Systems, 2009. ICEMS 2009. International Conference on*, 2009, pp. 1–6.
- [28]. R. Semken, M. Polikarpova, P. Roytta, J. Alexandrova, J. Pyrhonen, J. Nerg, A. Mikkola, and J. Backman, "Direct-drive permanent magnet generators for high-power wind turbines: benefits and limiting factors," *Renewable Power Generation, IET*, vol. 6, no. 1, pp. 1–8, 2012.
- [29]. M. Barcaro, N. Bianchi, and F. Magnussen, "Remarks on torque estimation accuracy in fractional-slot permanent-magnet motors," *Industrial Electronics, IEEE Transactions on*, vol. 59, no. 6, pp. 2565–2572, 2012.